KERNFORSCHUNGSZENTRUM

KARLSRUHE

Januar 1971

KFK 1357

Institut für Experimentelle Kernphysik

Differential Cross Section and Vector Polarization for the Elastic Scattering of 41 to 51 MeV Deuterons on Carbon

W. Fetscher, K. Sattler, N. C. Schmeing, E. Seibt, R. Staudt,
Ch. Weddigen, K. Weigele

GESELLSCHAFT FUR KERNFORSCHUNG M. B. H.

KARLSRUHE

KERNFORSCHUNGSZENTRUM KARLSRUHE

Januar 1971 KFK 1357

Institut für Experimentelle Kernphysik

Differential Cross Section and Vector Polarization for the Elastic Scattering of 41 to 51 MeV Deuterons on Carbon+

W. Fetscher, K. Sattler, N.C. Schmeing, E. Seibt, R. Staudt, Ch. Weddigen, and K. Weigele

Gesellschaft für Kernforschung m.b.H. Karlsruhe

+ Presented and submitted in part to "Third International Symposium on Polarization Phenomena in Nuclear Reactions", Madison, Wisconsin, 1970

Abstract

Differential cross section and vector polarization for the elastic scattering of 41, 46 and 51 MeV-deuterons on ^{12}C were obtained from single and double scattering experiments at the Karlsruhe isochronous cyclotron. Tensor polarization effects were found to be small. The experimental data are compared with the results of optical model calculations. Best fits to the polarization data are obtained with volume spin-orbit-terms for the deuteron optical potential.

Der differentielle Wirkungsquerschnitt und die Vektorpolarisation wurden für die elastische Streuung von 41, 46 und 51 MeV Deuteronen an ^{12}C durch Einfach- und Doppelstreuexperimente am Karlsruher Isochronzyklotron ermittelt. Tensorpolarisationseffekte erwiesen sich als vernachlässigbar. Die experimentellen Werte werden mit Ergebnissen von Optischen Potential-Rechnungen verglichen. Volum-Spin-Bahn-Terme im Optischen Potential für die Deuteronen geben die Polarisationswerte am besten wieder.

The elastic scattering cross section of deuterons on carbon was measured at energies of 41, 46 and 51 MeV. The vector polarization was obtained from double scattering experiments.

Both kinds of experiments were performed on the Karlsruhe fixed energy cyclotron using the same experimental set-up[1] (fig. 1). It consists of a first scattering chamber and a movable arm bearing a quadrupole triplet and a second rotating scattering chamber. For cross section measurements the movable arm is positioned at 0° and the first target is replaced by a circular aperture of down to 1 mm diam. Energies were degraded by Be and Al foils.

During the polarization experiments counting rates N after the second scattering were observed at azimuthal angles ϕ = 0, 90, 180, and 270° yielding asymmetry coefficients A, B, and C defined by

$$N \sim 1 + A\cos\phi + B\cos 2\phi + C\sin\phi .$$

The up-down asymmetry C gives a test for spurious asymmetries. We obtained an average value $\overline{C} = -0.84 \pm 1.65 \times 10^{-3}$ with χ^2 = 61.1 for 36 degrees of freedom. From this a root mean square value of $\pm 7.7 \times 10^{-3}$ for spurious asymmetries can be deduced.

The $\cos 2\phi$ term B which contains tensor polarizations was also found to be small[4] (fig.2). The average value $\overline{B}$ = $-4.22 \pm 1.38 \times 10^{-3}$ with $\chi^2 = 61.6$ for 36 degrees of freedom leads to a root mean square asymmetry of $\pm 7.2 \times 10^{-3}$ in B due to tensor polarization coefficients [5] T_{22}. We assume tensor polarization coefficients T_{20} and T_{21} to have an influence of the same order of magnitude.

If we neglect these small tensor polarization effects, one gets a right-left asymmetry

$$A = 2\,(iT_{11})_1\,(iT_{11})_2$$

and the vector polarization quantities [5] for the scattering from the two targets can be extracted from a calibration experiment. This we did at the energy pairs (51,46), (46,41) and (51,41) MeV (fig. 3). The sign of iT_{11} was deduced from optical model calculations.

Our differential cross section measurements extended experimental data [6,7] for 51 MeV to smaller and larger angles. We degraded the primary beam energy for additional measurements at 46 and 41 MeV. The experimental results for both cross sections and vector polarizations are shown in fig. 4. Numerical values with relative and absolute errors for differential cross section and vector polarizations are given in tables I and II.

We thank G.R. Satchler for fitting the cross section at 51 MeV using the search code "Hunter" [8] for optical model calculations. With a surface spin orbit term 4.2 MeV deep Satchler predicted polarizations (dashed curves in fig. 4). Using a code of B.A. Robson's we did not find much improvement when we varied the parameters of the surface ls term. Particularly the minimum in iT_{11} near 44^{o} could not be fitted. Hence we considered what effects might be relevant at 51 MeV as opposed to lower energies.

Since at higher energies deuterons see more of the inner part of the nucleus [9] and spin orbit forces become larger due to higher angular momenta, the Thomas form of the ls potential may no longer be justified [10]. Retaining Satchler's central terms we tried a volume ls potential with a factor of 5.5 MeV. In addition we introduced a small surface absorptive ls potential 0.1 MeV deep which is proportional to the imaginary central term. Its sign was chosen so that for $j=l+1$ one gets more interaction with the nucleus. The effects of these changes are: The volume ls potential indeed lowers the 44^{o} minimum and the ls absorption gives a minimum in the cross section near 150^{o}.

Very recently J. Raynal [11] fitted the cross section and polarization data for 51 MeV using his search code "Magali" [12] with a Thomas-form ls potential. Weighting the polarization data by a factor of 20 and starting from different parameter sets, Raynal gets ambiguities in the central potential terms (Raynal I and V in fig. 5). Independently of these ambiguities he obtains negative radii for the surface ls potential, which is equivalent to an exponential volume ls potential.

The fits to the cross section at 51 MeV based on search codes (curves 1 and 3 in fig. 6) are better than the result of the present calculations (curve 2) as was to be expected.

Fig. 7 shows the corresponding fits to the deuteron polarization and compares the optical potentials used. For carbon the Thomas form (potential 1) gives a volume ls potential also, but it seems not to be voluminous enough.

We expect that further polarization experiments at higher energies could test whether volume ls potentials are physically meaningful.

We thank Dr. J. Raynal for sending us results of optical model calculations prior to publication. We are indebted to Dr. G. Schatz and his staff for the supply of the cyclotron beam.

References:

1) E. Seibt and Ch. Weddigen, to be published in Nucl. Instr. and Meth.

4) E. Seibt, Ch. Weddigen, and K. Weigele, Phys. Lett. 29B (1968) 567

5) W. Lakin, Phys. Rev. 98 (1954) 139

6) U. Schmidt-Rohr et al., Nucl. Phys. A111 (1968) 1333

7) H. Brückmann et al., private communication (1968)

8) R. H. Bassel, R.M. Drisko, and G. R. Satchler, ORNL-3240

9) B. Tatischeff and I. Brissaud, to be published

10) F. G. Perey, Second Polarization Symp., Karlsruhe (1965) 191

11) J. Raynal, private communication

12) J. Raynal, Technical Report DPh-T/69-42, Saclay (1969)

Table I: Differential Cross Section with relative and absolute errors for the elastic Scattering of 41, 46, and 51 MeV-deuterons on ^{12}C.

E_d = 41 MeV

θ_{CM}/deg	$\frac{d\phi}{d\Omega}/\frac{mb}{sr}$	θ_{CM}/deg	$\frac{d\phi}{d\Omega}/\frac{mb}{sr}$	θ_{CM}/deg	$\frac{d\phi}{d\Omega}/\frac{mb}{sr}$
11.71	1.75×10^{3}	44.1	2.88×10^{1}	96.8	1.31×10^{0}
12.88	1.42	46.3	2.15	97.8	1.29
14.05	1.11	48.6	1.79	99.8	1.15
15.21	8.49×10^{2}	50.8	1.53	101.8	9.99×10^{-1}
16.38	6.14	53.1	1.44	103.8	8.36
17.55	4.30	55.3	1.55	105.8	6.70
18.71	2.79	57.5	1.49	107.7	5.83
19.88	1.75	59.8	1.36	109.7	5.16
21.05	9.37×10^{1}	62.0	1.34	111.6	4.27
22.21	4.43	64.2	1.21	113.5	3.10
23.37	1.44	66.4	1.03	115.5	2.58
24.52	5.47×10^{0}	68.5	8.41×10^{0}	117.4	2.00
25.68	6.11	7.07	6.61	119.3	1.62
26.85	1.40×10^{1}	72.9	6.04	123.9	1.06
28.00	2.61	75.0	4.81	128.5	8.08×10^{-2}
29.16	3.77	77.1	3.82	133.0	7.57
30.3	4.81	79.3	3.23	137.5	6.78
31.5	5.89	81.4	2.73	141.9	5.56
32.6	6.66	83.5	2.30	146.3	4.36
33.8	6.85	85.6	2.05	150.6	3.76
34.9	6.79	87.6	2.19	152.3	3.98
37.2	6.19	89.7	1.93	154.9	3.90
39.5	5.04	91.8	1.83	159.1	4.92
41.8	3.81	93.8	1.51	163.5	6.28
		95.8	1.49	167.5	7.95

Relative Error: < 10 %   Absolute Error: < 20 %

E_d = 46 MeV

11.71	1.80×10^{3}	44.1	2.80×10^{1}	95.8	7.65×10^{-1}
12.88	1.37	46.3	2.09	97.9	6.68
14.05	1.06	48.6	1.74	99.9	5.30
15.21	7.70×10^{2}	50.8	1.63	101.8	4.31
16.38	5.05	53.1	1.50	103.8	3.56
17.55	3.35	55.3	1.42	105.8	3.11
18.71	2.07	57.5	1.32	107.8	2.70
21.05	5.72×10^{1}	59.8	1.18	109.7	2.17
22.21	2.42	62.0	1.06	111.6	1.72
23.37	1.13	64.2	8.83×10^{0}	113.6	1.33
23.94	1.09	66.4	7.09	115.5	1.13
24.52	1.36	68.5	5.63	119.3	7.40×10^{-2}

Table I, E_d = 46 MeV continued

θ_{CM}/deg	$\frac{d\phi}{d\Omega}/\frac{mb}{sr}$	θ_{CM}/deg	$\frac{d\phi}{d\Omega}/\frac{mb}{sr}$	θ_{CM}/deg	$\frac{d\phi}{d\Omega}/\frac{mb}{sr}$
25.68	2.30	70.7	4.50	123.9	5.12
26.85	3.99	72.9	3.57	128.5	3.98
28.00	5.20	75.0	2.86	133.0	3.39
29.16	6.73	77.1	2.30	141.9	2.26
30.3	7.52	79.3	1.97	146.3	1.89
31.5	8.09	81.4	1.80	150.6	1.75
32.6	8.23	83.5	1.51	154.9	1.60
33.8	8.32	85.6	1.40	159.1	1.78
34.9	7.94	87.6	1.20	163.5	2.18
37.2	6.64	89.7	1.08	167.5	2.63
39.5	5.22	91.8	9.53×10^{-1}		
41.8	3.77	93.8	9.17		

Relative Error: < 7 %   Absolute Error: < 15 %

E_d = 51 MeV

4.69	6.48×10^{3}	+33.7	8.41	+85.4	9.17×10^{-1}
5.86	4.95	+34.8	7.83	+87.4	7.86
7.02	4.51	+37.1	6.33	+89.5	6.86
8.20	3.13	+39.4	4.58	89.7	6.89×10^{-1}
9.37	2.73	40.7	4.17	+91.6	5.69
10.54	2.21	+41.7	3.53	+93.6	4.74
11.79	1.71	+43.9	2.31	+95.6	3.88
12.88	1.34	+45.1	2.07	+97.6	3.26
14.05	9.41×10^{2}	+46.2	1.88	+99.7	2.54
15.21	6.76	46.3	1.97	99.9	2.56
+15.80	5.53	+47.3	1.77	++102.7	1.79
16.38	4.37	+48.4	1.72	++104.7	1.45
+16.97	3.62	+49.6	1.63	++106.6	1.15
17.55	2.74	+50.7	1.60	++109.6	9.74×10^{-2}
+18.01	2.14	+51.8	1.49	109.7	9.15
18.71	1.64	+52.9	1.45	++111.5	7.25
+19.17	1.19	+54.0	1.41	++114.4	5.62
19.88	8.87×10^{4}	+55.2	1.30	117.2	4.30
+20.33	5.85	+57.4	1.17	++119.1	3.85
21.05	4.49	57.6	1.16	119.3	3.49
+21.49	3.07	+59.6	9.96×10^{0}	++121.0	3.13
22.21	2.39	+61.8	7.95	++123.8	2.78
+22.77	2.10	+64.0	6.53	123.9	2.76
+23.81	2.73×10^{1}	+66.2	5.13	++128.4	2.06
+25.08	3.88	+68.4	3.92	128.5	2.04
+26.24	5.47	+70.5	2.91	133.0	1.59
+27.40	6.96	+72.7	2.37	137.5	1.29
+28.55	8.03	+74.8	1.84	141.9	1.05
29.10	8.64	+76.9	1.61	146.3	9.20×10^{-3}
+29.59	8.78	+79.1	1.38	150.6	8.50
+30.2	9.28	79.3	1.41	154.9	9.10
+31.4	9.47	+81.2	1.19	159.1	1.11×10^{-2}
+32.5	9.16	+83.3	1.04		

Relative Error: < 5 %   Absolute Error: < 10 % [7]

+ Schmidt-Rohr et al. [6], ++ Brückmann et al.

Table II: Vector polarization iT_{11} for the elastic Scattering of 41, 46 and 51 MeV-deuterons on ^{12}C (Basel-Convention).

E_d = 41 MeV

θ_{CM}/deg	iT_{11}	θ_{CM}/deg	iT_{11}
15.2	-0.047 ± 0.012	34.9	-0.112 ± 0.018
17.4	-0.057 ± 0.010	37.8	-0.136 ± 0.020
21.1	-0.082 ± 0.015	40.6	-0.173 ± 0.027
22.7	-0.132 ± 0.019	42.9	-0.199 ± 0.025
24.6	-0.122 ± 0.024	44.4	-0.178 ± 0.023
26.4	-0.061 ± 0.021	48.6	-0.102 ± 0.018
29.1	-0.061 ± 0.022	53.0	+0.008 ± 0.013
32.0	-0.079 ± 0.015	57.5	+0.095 ± 0.018

E_d = 46 MeV

θ_{CM}/deg	iT_{11}	θ_{CM}/deg	iT_{11}
15.2	-0.007 ± 0.032	34.9	-0.115 ± 0.041
19.0	-0.067 ± 0.031	36.4	-0.157 ± 0.038
21.0	-0.128 ± 0.035	38.7	-0.159 ± 0.028
22.9	-0.148 ± 0.039	41.8	-0.182 ± 0.048
24.3	-0.148 ± 0.050	44.1	-0.239 ± 0.044
25.7	-0.048 ± 0.039	46.3	-0.116 ± 0.044
27.4	+0.023 ± 0.038	49.2	+0.012 ± 0.042
29.2	-0.050 ± 0.033	52.0	+0.149 ± 0.054
32.0	-0.096 ± 0.046	55.3	+0.134 ± 0.041
		57.5	+0.176 ± 0.033

E_d = 51 MeV

θ_{CM}/deg	iT_{11}	θ_{CM}/deg	iT_{11}
19.9	-0.143 ± 0.035	38.7	-0.147 ± 0.020
21.6	-0.202 ± 0.028	43.2	-0.165 ± 0.024
23.4	-0.101 ± 0.036	46.1	+0.006 ± 0.021
26.3	+0.009 ± 0.023	49.9	+0.136 ± 0.022
28.1	+0.046 ± 0.030	54.2	+0.318 ± 0.035
33.2	-0.080 ± 0.027	57.5	+0.324 ± 0.038
36.3	-0.130 ± 0.026	62.9	+0.328 ± 0.040

Figure Captions:

Fig. 1: Experimental set-up used for cross section measurements (top) and double scattering experiments (bottom). Q,L, = quadrupole lenses, S = movable scintillation screens, T = targets, C = counter telescopes (combinations of surface barrier and scintillation counters), M = monitors (scintillation counters), FK = Faraday-cup, SK = scattering chambers.

Fig. 2: The cosϕ-term A and the cos2ϕ-term B for double scattering of 51 MeV deuterons on carbon as a function of the secondary scattering angle θ_{2CM}. $E_{1,2}$ = energies at the two targets.

Fig. 3: Calibration experiments for deducing the vector polarization quantities $(iT_{11})_n$ from the right-left asymmetries A_n. The sign of iT_{11} is deduced from calculations.

Fig. 4: Differential cross section and vector polarization iT_{11} (Basel convention) at 51, 46, and 41 MeV. Dashed lines: Satchler prediction from a search on differential cross section at 51 MeV alone; solid lines: present calculations.

Fig. 5: Definition and values (in MeV and f) of the optical potential parameters for fits shown in this paper. Set 1 was obtained by a search on the differential cross section at 51 MeV alone with a preset value of V_{soS}. The parameter sets of Raynal's are results of a search on differential cross section and vector polarization at 51 MeV with different starting parameter sets; for positive radii these potentials differ in the ls terms only by about 20 %.

Fig. 6: Optical model fits to the differential cross section at 51 MeV. The numbers of the curves refer to the parameter sets in fig. 5.

Fig. 7: Radial dependence of the optical potentials and corresponding fits to the vector polarization iT_{11} at 51 MeV. The numbers of the diagrams and curves refer to the parameter sets in fig. 5. The lower part of the potential diagrams gives the real volume and absorptive surface parts of the central potential. The upper part represents the spin orbit potential divided by -(ls). Note the difference in potential scales.

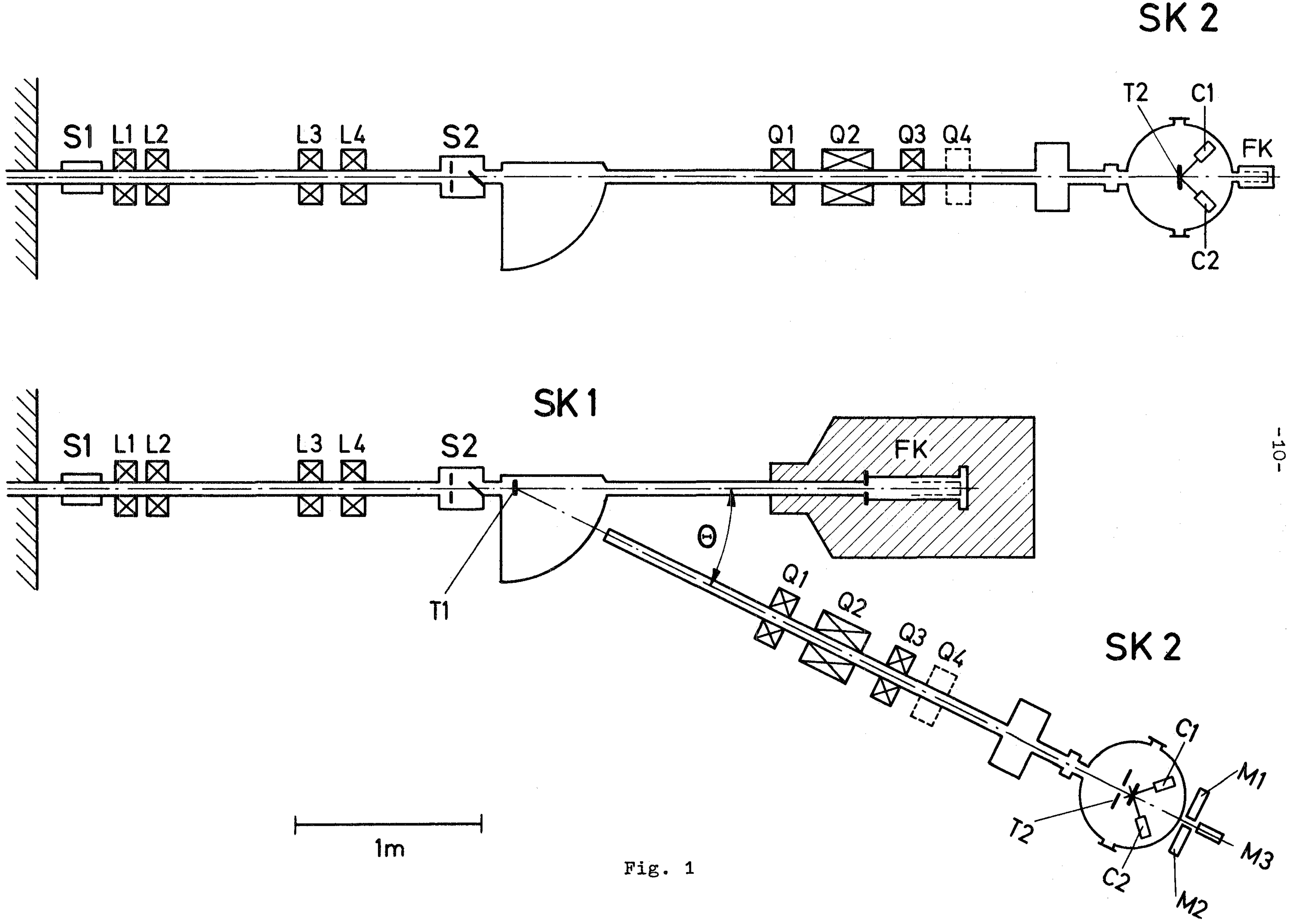
SK 2
S1
L1
L2
L3
L4
S2
Q1
Q2
Q3
Q4
T2
C1
C2
FK
SK 1
S1
L1
L2
L3
L4
S2
FK
Θ
T1
Q1
Q2
Q3
Q4
SK 2
C1
M1
T2
M3
C2
M2
1m

Fig. 1

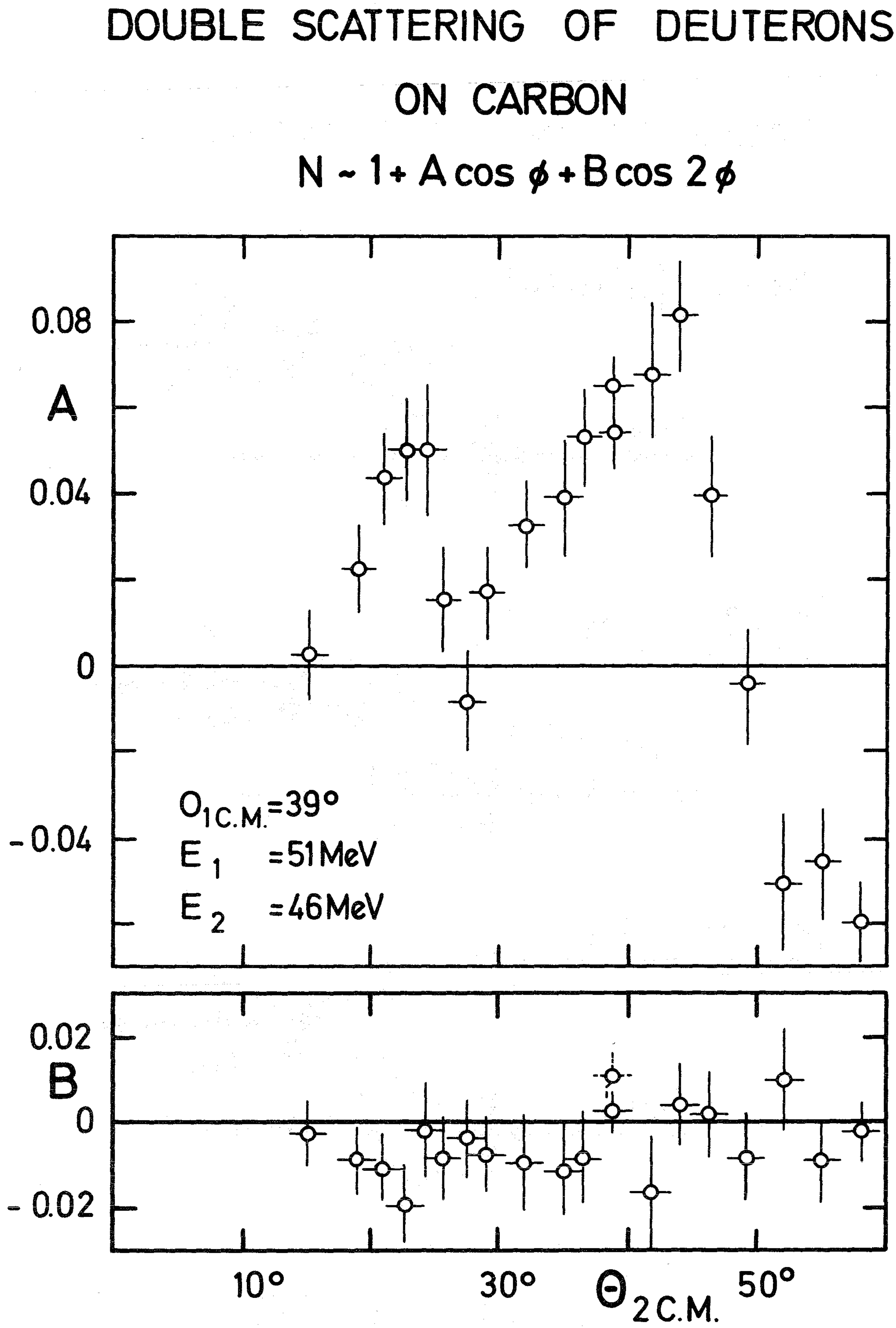
DOUBLE SCATTERING OF DEUTERONS
ON CARBON
N ~ 1+ A cos ϕ + B cos 2ϕ
0.08
A
0.04
0
- 0.04
Θ1C.M.=39°
E 1 =51MeV
E 2 =46MeV
0.02
B
0
- 0.02
10°
30°
Θ2C.M.
50°

Fig. 2

CALIBRATION EXPERIMENT

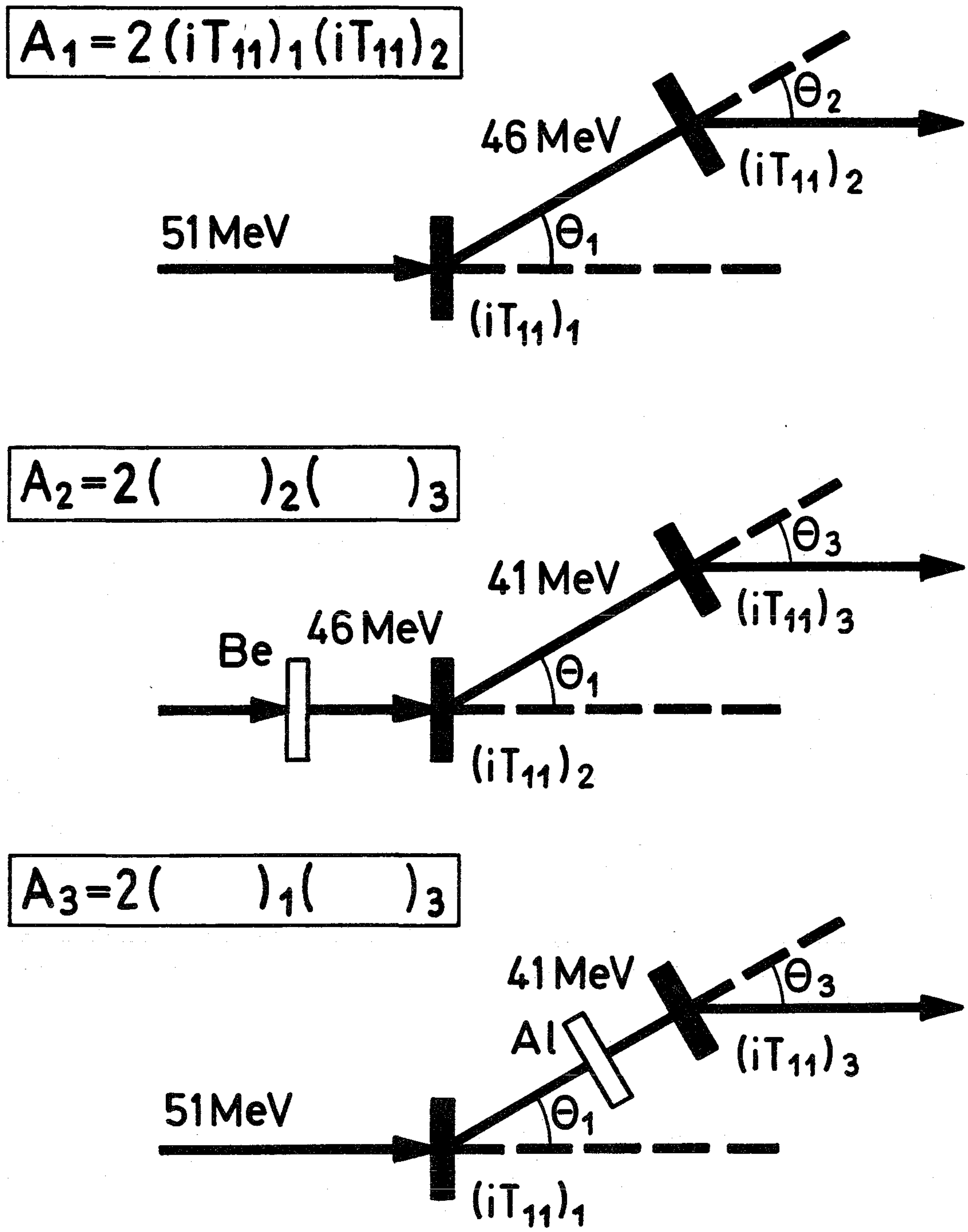

$$(iT_{11})_1 = \pm\sqrt{A_1 A_3 / 2A_2}$$

Fig. 3

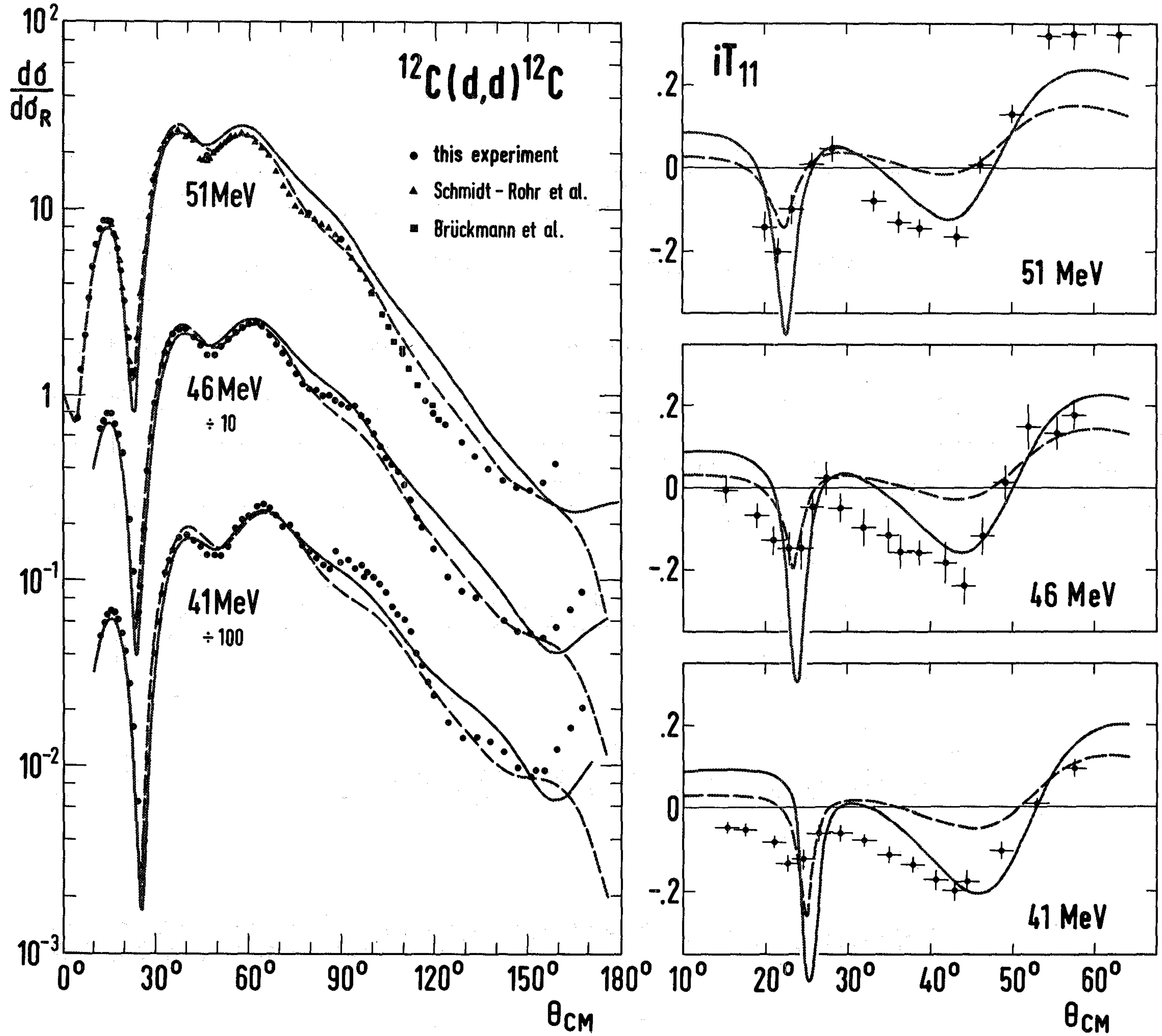

$^{12}C(d,d)^{12}C$
this experiment
Schmidt - Rohr et al.
Brückmann et al.
51MeV
46MeV
÷ 10
41MeV
÷ 100
$\frac{d\sigma}{d\sigma_R}$
10^2
10
1
10^{-1}
10^{-2}
10^{-3}
0° 30° 60° 90° 120° 150° 180°
θ_{CM}
iT_{11}
.2
0
-.2
51 MeV
46 MeV
41 MeV
10° 20° 30° 40° 50° 60°
θ_{CM}

Fig. 4

OPTICAL POTENTIAL, 51 MeV-Deuterons on CARBON

$$V(r) = V_C - V_o\, f_o - 4iW_D \frac{d}{dr} f_D - \left[\left(\frac{h}{m_\pi c}\right)^2 V_{soS} \frac{1}{r} \frac{d}{dr} f_{so} + V_{soV}\, f_o + 4iW_{so} \frac{d}{dr} f_D \right] \quad (1\ s)$$

$$f_k = \frac{1}{1 + \exp\left((r - r_k A^{1/3})/a_k \right)}$$

	V_o	r_o	a_o	W_D	r_D	a_D	V_{soS}	r_{so}	a_{so}	V_{soV}	W_{so}
1 Satchler	86,0	1.024	0.766	8.25	1.343	0.757	4.16	1.024	0.766	-	-
2 present calculation	86.0	1.024	0.766	8.25	1.343	0.757	-	-	-	5.5	0.01
3 Raynal V	75.5	1.166	0.760	10.58	1.111	0.857	307.50	-2.264	1.575	-	-
Raynal I	105.8	0.867	0.891	8.80	1.311	0.810	125.89	-1.310	1.454	-	-

Fig. 5

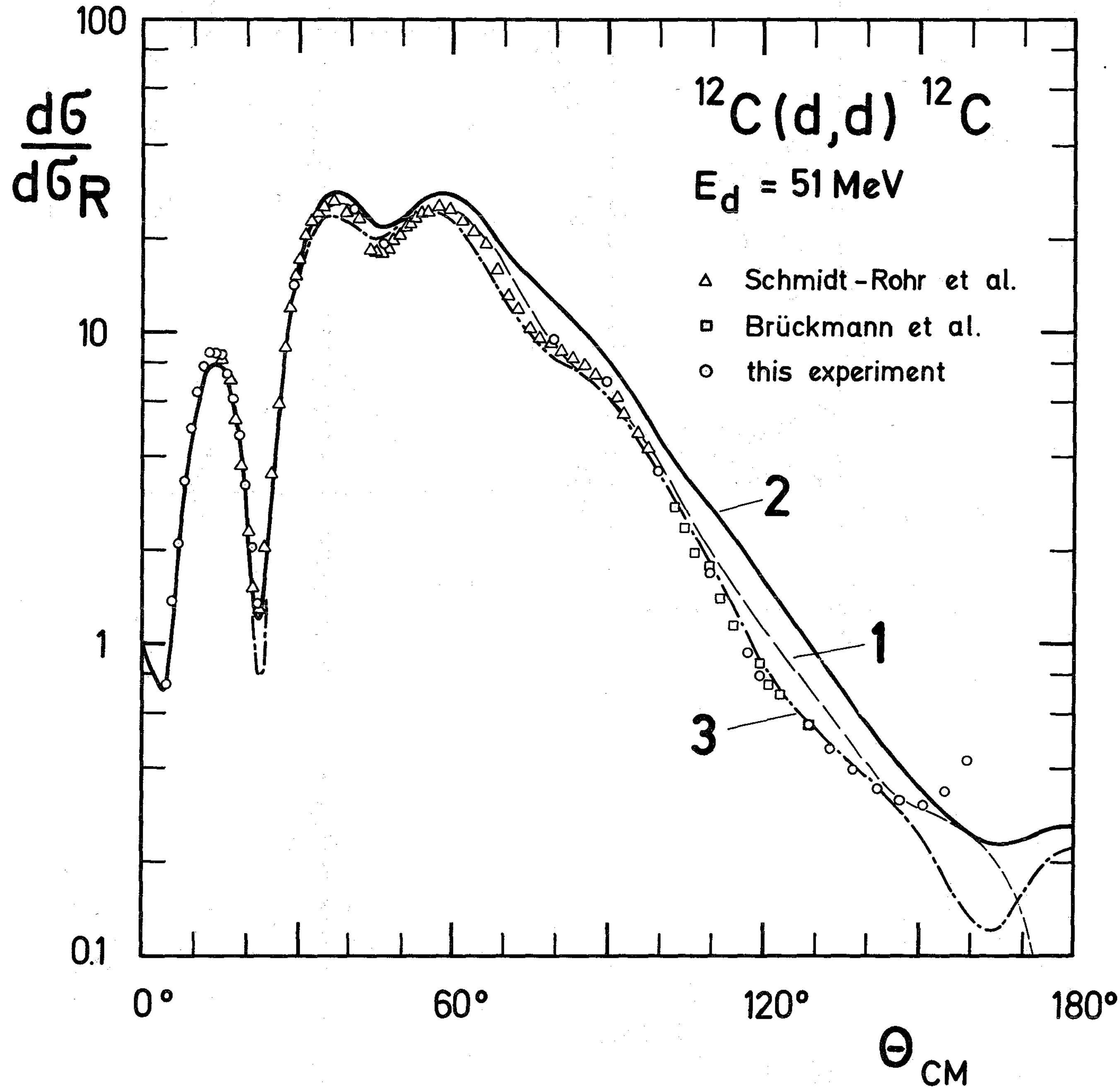
100
10
1
0.1
$\frac{d\sigma}{d\sigma_R}$
$^{12}C(d,d)\ ^{12}C$
E_d = 51 MeV
△ Schmidt-Rohr et al.
□ Brückmann et al.
○ this experiment
2
1
3
0°
60°
120°
180°
Θ_{CM}

Fig. 6

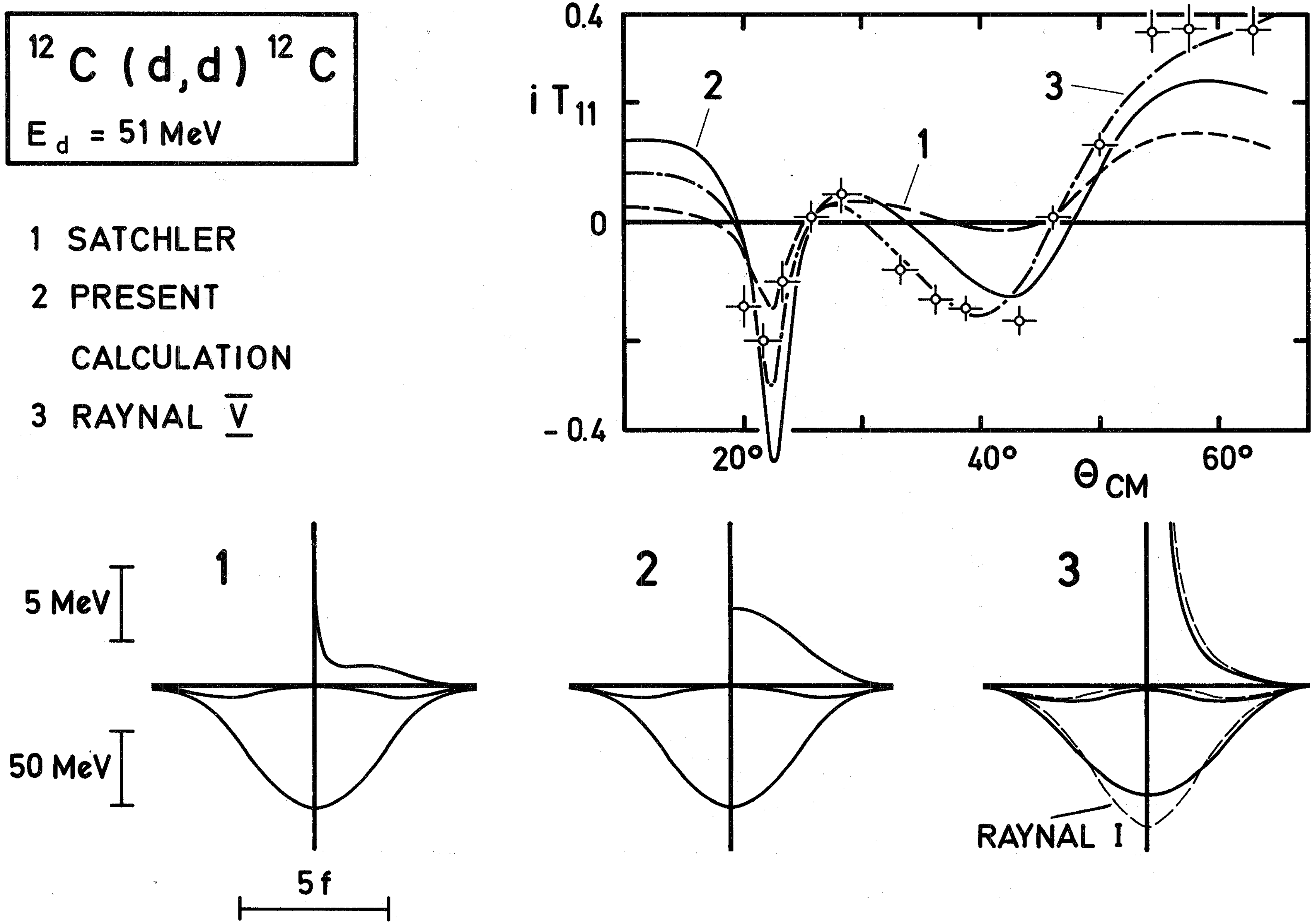

$^{12}C\ (d,d)\ ^{12}C$
E_d = 51 MeV
1 SATCHLER
2 PRESENT CALCULATION
3 RAYNAL $\overline{V}$
0.4
iT_{11}
0
- 0.4
20°
40°
60°
Θ_{CM}
1
2
3
5 MeV
50 MeV
5 f
RAYNAL I

Fig. 7